Influence of ADP on Cross-Bridge-Dependent Activation of Myofibrillar Thin Filaments

Dahua Zhang, Kyle W. Yancey, and Darl R. Swartz
Department of Anatomy and Cell Biology, Indiana University Medical School, Indianapolis, Indiana 46202 USA

ABSTRACT   Contraction of skeletal muscle is regulated by calcium at the level of the thin filament via troponin and tropomyosin. Studies have indicated that strong cross-bridge binding is also involved in activation of the thin filament. To further test this, myofibrils were incubated with a wide range of fluorescent myosin subfragment 1(fS1) at pCa 9 or pCa 4 with or without ADP. Sarcomere fluorescence intensity and the fluorescence intensity ratio (non-overlap region/overlap region) were measured to determine the amount and location of bound fS1 in the myofibril. There was lower sarcomere fluorescence intensity with ADP compared to without ADP for both calcium levels. Similar data were obtained from biochemical measures of bound fS1, validating the fluorescence microscopy measurements. The intensity ratio, which is related to activation of the thin filament, increased with increasing [fS1] with or without ADP. At pCa 9, the fluorescence intensity ratio was constant until 80–160 nM fS1 without ADP conditions, then it went up dramatically and finally attained saturation. The dramatic shift of the ratio demonstrated the cooperative character of strong cross-bridge binding, and this was not observed at high calcium. A similar pattern was observed with ADP in that the ratio was right-shifted with respect to total [fS1]. Saturation was obtained with both the fluorescence intensity and ratio data. Plots of intensity ratio as a function of normalized sarcomere intensity (bound fS1) showed little difference between with and without ADP. This suggests that the amount of strongly bound fS1, not fS1 state (with or without ADP) is related to activation of the thin filament.

INTRODUCTION

Regulation of contraction in striated muscle involves calcium binding to troponin followed by changes in the actin-tropomyosin interaction, allowing for actomyosin interactions and contraction. The steric-hindrance model was proposed to explain the molecular mechanisms of activation. It proposes that calcium binding to troponin moves tropomyosin to a position that does not block the interaction of actin and myosin (reviewed in Squire and Morris, 1998). While the early x-ray diffraction studies that gave rise to this hypothesis were highly model-dependent, more recent studies using electron micrographic methods generally support a model based upon tropomyosin movement (Lehman et al., 1994; Vibert et al., 1997; Xu et al., 1999). Biochemical studies show calcium-dependent changes between troponin I and actin (Tao et al., 1990; Miki and Iio, 1993) but not tropomyosin and actin (Tao et al., 1983; Miki et al., 1998). Conformation changes in tropomyosin at the troponin binding site are not sensitive to calcium binding (Ishii and Lehrer, 1990), while changes outside the troponin binding region are calcium-sensitive (Farah and Reinach, 1999).

An alternative model (reviewed in Chalovich, 1992) has been proposed for the regulation of contraction based upon biochemical (Chalovich and Eisenberg, 1982) and mechanical (Brenner, 1988) studies. In this model, calcium regulates the kinetics of a step in the actomyosin ATPase pathway. The phosphate release step was proposed as the calcium-sensitive step (Chalovich and Eisenberg, 1982), yet studies with caged phosphate show little change in rate with altered calcium (Millar and Homsher, 1990; Walker et al., 1992). The calcium sensitivity of tension redevelopment is dramatically reduced by treatment of skinned fibers with N-ethylmaleimide-modified S1, suggesting that the change in kinetics is the result of strong cross-bridge activation of the thin filament (Swartz and Moss, 1992). However, recent skinned fiber studies using a conformationally sensitive fluorescent probe on troponin I (Brenner et al., 1999) show that the kinetics of troponin I fluorescence change are much faster than tension redevelopment, and thus not limiting the rate of tension redevelopment (Brenner and Chalovich, 1999). Thus, whether calcium regulation is via rate of cross-bridge cycling (kinetic) or number of cycling cross-bridges (steric) is yet to be resolved. In vitro motility studies using regulated actin filaments show both changes in the number of filaments moving and their speed as a function of calcium (Homsher et al., 1996; Gordon et al., 1997), which does not fully resolve the kinetic/steric debate on thin filament regulation.

Independent of the detailed mechanism of calcium regulation, strong binding of cross-bridges plays a role in the process. The structural and biochemical data, which do not agree on calcium-induced movement of tropomyosin, do agree that strong-binding cross-bridges (or S1) cause a movement of tropomyosin. Structural studies (Popp and Maéda, 1993; Vibert et al., 1997) suggest that tropomyosin is moved from near the periphery of the actin helix toward the groove upon the binding of strong cross-bridges. The distribution of fluorescent S1 binding in rigor myofibrils

also supports the idea that rigor cross-bridges activate the thin filament (Swartz et al., 1990), while calcium alone does not fully activate the thin filament for rigor S1 binding (Swartz et al., 1996). Biochemical data show that there is a conformational (Ishii and Lehrer, 1990) and positional change (Graceffa, 1999) in tropomyosin associated with strong cross-bridge binding. A two-state model was proposed by Hill et al. (1980) with calcium and/or strong cross-bridge binding, shifting the thin filament from the weak to strong binding state. Detailed analysis at both the biochemical and structural level of calcium and strong cross-bridge-induced movement of tropomyosin has led to the proposal of three different states of the thin filament (McKillop and Geeves, 1993; Vibert et al., 1997). The biochemical states (McKillop and Geeves, 1993; Head et al., 1995; Maytum et al., 1999) are defined as blocked, closed, and open. Structurally, the three states are related to different positions of tropomyosin at no-calcium, high-calcium, and with strongly bound myosin heads (Vibert et al., 1997). A question that remains is the contribution of changes in troponin position to the proposed changes in tropomyosin based upon structural studies (Lehrer, 1994; Squire and Morris, 1998).

To test the hypothesis that strong binding cross-bridges are involved in shifting the thin filament into the "on" or open state, we investigated the amount and distribution of fluorescently labeled myosin subfragment 1(fS1) in myofibrils with and without ADP at high and low calcium. There are several advantages to this approach in that we use the native thin filament, can monitor the distribution at very low levels of fS1, and can compare the (−) and (+) ADP state of the myosin head. Comparing (−) and (+) ADP allows for testing whether the state of the strongly bound cross-bridge influences the closed-to-open transition. A feature of the McKillop and Geeves and Hill models is that the nucleotide state of S1 does not influence the closed/open (off/on) equilibrium. The current study validates our previous studies and supports the idea that strong cross-bridge binding has a dominant role in thin filament activation, while the nucleotide state of the strong binding cross-bridge has little influence on the closed/open (off/on) equilibrium.

MATERIALS AND METHODS

Proteins

Myofibrils (rabbit psoas) and myosin (bovine cutaneous trunci) were prepared as described in Swartz et al. (1990). Myosin subfragment 1 was prepared using chymotryptic digestion, and the S1 was purified on SP-Sephadex, as described in Swartz and Moss (1992). Fluorescent S1 (fS1) was prepared as described in Swartz et al. (1996) with Texas Red C2 maleimide (Molecular Probes, Inc., Eugene, OR). The labeled protein was stored as an ammonium sulfate pellet at 4°C. Before use, the protein was desalted on a Sephadex G-25 column equilibrated with pCa 9 or 4 buffer (see below) with 1 mM DTT.

Solutions

Calcium buffers were made by mixing stock solutions of pCa 9.0 and 3.0. The base solution was 20 mM PIPES (pH 7.0), 4 mM $MgCl_2$ (free), 4 mM EGTA, 1 mM NaN_3, KCl to yield 200 mM ionic strength, and $CaCl_2$ to yield the desired free calcium concentration. The stability constants listed by Godt and Lindley (1982) and Fabiato's program (1988) were used to determine the concentrations of total $MgCl_2$ and $CaCl_2$ needed to achieve the desired free ion concentrations.

Binding studies

Myofibrils (0.25 mg/ml final) were mixed with different levels of fS1 (0.1–7680 nM) in either pCa 9.0 or pCa 4.0 buffer containing 1 mM DTT and 1 mg/ml BSA under either (+) or (−) ADP (4 mM final) conditions. Contaminating ATP was removed from the ADP by pretreatment of stock ADP (20 mM) with 20 mM glucose and hexokinase (10 units/ml) for 30 min. The incubation solution also contained 200 μM di(adenosine) pentaphosphate to inhibit the intrinsic myokinase activity, which could convert ADP to ATP and AMP. Without the di(adenosine) pentaphosphate, the myofibrils with ADP shortened independent of calcium. The myofibril/fS1 mixture was incubated for 4 h at room temperature in the dark, then 100 μl solution was spread on a coverslip and fixed with 3% formaldehyde in the same buffer as the incubation buffer without fS1. The coverslips were rinsed with pCa 9.0 or 4.0 buffer, then mounted on 75% glycerol, 20 mM Tris (pH 8.5), 2 mM $MgCl_2$, 2 mM EGTA, 1 mM NaN_3, 1 mg/ml p-phenylenediamine and sealed with nail polish. The slides were stored at −20°C until observation.

Imaging

Myofibrils were imaged using a Zeiss Axiovert TV (Thornwood, NJ) epifluorescence microscope equipped with a 100× oil-immersion phase contrast lens (NA 1.3), and a narrow-bandpass Texas Red filter. Digital images were obtained with 12-bit resolution using a CCD (KAF 1300 chip, Photometrics Inc., Tucson, AZ) controlled by a Matrox board using IPLab Spectrum software (v3.0, Signal Analytics, Vienna, VA) run by a Macintosh 840AV. The images were obtained by first acquiring the phase contrast image and then the fluorescence image. The wide dynamic range of fS1 levels required the use of different exposure times and a neutral density filter in the excitation pathway to prevent saturation of the camera at high fS1 levels. Sarcomeric fluorescence intensity data were corrected to compensate for these variations in imaging. IPLab Spectrum software was used for image processing and analysis of fluorescence intensity data. Sarcomere fluorescence intensity and the fluorescence intensity ratio (non-overlap/overlap) were measured as described in Swartz et al. (1996) with minor modifications. The spacing from the Z-line to the non-overlap and overlap window was 0.31 and 0.89 μm, respectively, for the shorter-length thin filaments of rabbit psoas myofibrils. Fluorescence intensity and fluorescence intensity ratio data represent the mean of 18–20 myofibrils per treatment using three contiguous, in-focus sarcomeres per myofibril. For visual presentation, the 12-bit myofibril images were rotated to the horizontal with bilinear interpolation and cropped such that a Z-line was in the center of the image. Fluorescence images are presented in 8-bit and individually normalized to demonstrate the fluorescent pattern, not the fluorescence intensity.

Assays

Myofibrillar protein was determined using the biuret assay (Gornall et al., 1949), S1 concentration using UV absorbance, and fS1 using the bicinchoninic acid assay (Hill and Straka, 1988) with S1 as the standard. The amount of fS1 bound to myofibrils was measured both by a biochemical method and by image analysis using fluorescence intensity. Biochemical

analysis was done as described in Swartz et al. (1996) using the NH_4/ EDTA ATPase assay. The P_i assay of Carter and Karl (1982), with minor modifications (Swartz et al., 1999), was used to determine ATPase activity. Standard curves were made using fS1 to determine the free and total fS1. Bound fS1 was determined by subtracting free activity from total activity. Myofibrils samples without fS1 were processed in the same fashion to correct for residual myofibrils in the supernatant. Reagents were from Sigma Chemical Co. (St. Louis, MO) unless specified otherwise.

RESULTS

In initial studies, ADP was pretreated with glucose and hexokinase to remove contaminating ATP. Without this pre-treatment, the myofibrils shortened rapidly upon addition of ADP. With this treatment, acute sarcomere shortening was not observed, but a slow decrease in sarcomere length occurred, which was inversely related to the fS1 level (higher fS1 gave less sarcomere shortening). To eliminate this problem, di(adenosine) pentaphosphate (a myokinase inhibitor) was added to myofibrils before addition of ADP, incubated for 4 h with ADP, then sarcomere length was analyzed. This showed that, at 200–400 μM di(adenosine) pentaphosphate, the sarcomere length was essentially the same as (−)ADP controls (2.78 μm, data not shown). Lower concentrations resulted shorter sarcomere lengths with no inhibitor, giving a sarcomere length of 2.58 μm. For all subsequent experiments, 200 μM di(adenosine) pentaphosphate was included to inhibit ATP production from myokinase. Similar observations on the influence of ATP contamination (both direct and indirect via myokinase) have been noted in skinned fiber preparations (Horiuti et al., 1997).

The amount of bound fS1 was determined biochemically by measuring the free fS1 level in the supernatant using the NH_4/EDTA ATPase assay with fS1 as the standard. The conditions were the same as those used for samples prepared for fluorescence microscopy. Fig. 1 shows the relationship between total and bound fS1 at pCa 4 and 9 either with or without ADP. Globally, the amount of bound fS1 saturated at fS1 levels >2.5 μM. Without ADP, there was no difference between the amount bound at high and low calcium, while with ADP there was a difference at the lowest fS1 level. Addition of ADP resulted in less fS1 bound at levels below 2 μM, as would be expected for the 10–50-fold weaker binding of S1-ADP to actin compared to without ADP (McKillop and Geeves, 1991). The biochemical methods show that ADP influenced the amount bound, while calcium had little influence on the amount bound with or without ADP. This method does not give information on the location of fS1 binding within the myofibril.

The distribution of the bound fS1 at high/low calcium with and without ADP was observed using fluorescence microscopy. Fig. 2 shows the distribution of fS1 at select levels of fS1 at pCa 9 and pCa 4 without ADP to demonstrate the differences in distribution. The distribution of fS1 at pCa 9.0 changed dramatically with increased fS1; at low
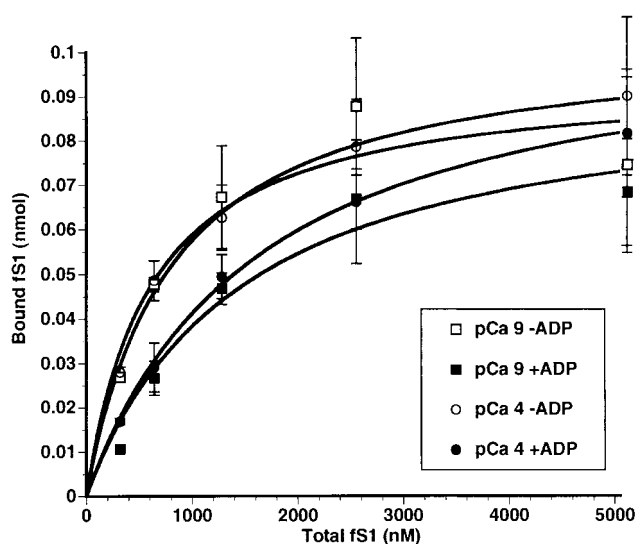

FIGURE 1 Fluorescent S1 binding to myofibrils measured by ATPase activity. Myofibrils at pCa 9 (*squares*) or 4 (*circles*) and with (*filled*) or without (*open*) ADP were incubated with different levels of fS1. Bound fS1 was removed by centrifugation and free fS1 was determined by ATPase activity in the supernatant. Data points represent the mean ± SD ($n = 4$). Note that there was little difference between pCa 9 and 4, while (+) ADP gave less bound than without ADP at low levels of fS1.

concentration (40 nM), fS1 was bound predominantly in the overlap region and changed to the non-overlap region at higher levels. At pCa 4.0, there was little apparent change in distribution with increased [fS1], with the fS1 being preferentially in the non-overlap region. Lower levels of fS1 at pCa 4.0 resulted in most of the fS1 in the overlap region (images not shown, see Fig. 5 below and Swartz et al., 1996, Fig. 4). Fig. 3 shows the influence of ADP on fS1 distribution at pCa 9.0. The change in distribution of fS1 with increased levels of fS1 with ADP lagged behind that without ADP, but both patterns were similar at 2.5 μM. At pCa 4.0, the influence of ADP was not visually apparent (images not shown).

To determine the amount and distribution of fS1, we measured the sarcomeric fluorescence intensity (amount) and ratio of the intensity in the non-overlap to the overlap region (distribution) using analytical fluorescence microscopy (Swartz et al., 1996, 1997). These methods reduce the visual images into numerical data, allowing for plots of the amount and distribution of fS1 as a function of fS1. Myofibrils were incubated with a wide range of fS1 levels (0.1–7680 nM) and imaged quantitatively using fluorescence microscopy. For this wide range, different exposure times and a neutral density filter were used to ensure that the dynamic range of the camera was not exceeded. Linearity of the camera with exposure time using fS1-treated myofibrils was confirmed (data not shown). The sarcomeric intensity data were corrected for exposure conditions and plotted on a log/log scale in Fig. 4. Globally, the sarcomeric fluores-
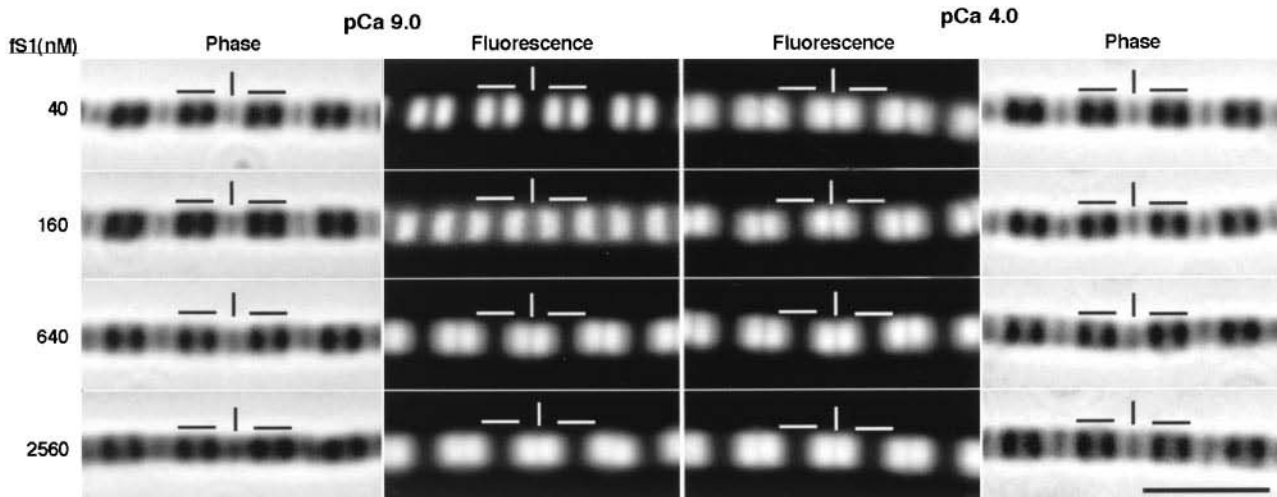
FIGURE 2 The pattern of fS1 binding is calcium dependent. Myofibrils at pCa 9 (*left two panels*) or 4 (*right two panels*) were incubated with different levels of fS1 (40, 160, 640, and 2560 nM) without ADP, fixed, then imaged. Outer panels are phase contrast and inner panels are fluorescence micrographs. The fluorescence images were processed to show the fluorescence pattern instead of intensity. Vertical lines note Z-lines and horizontal lines note A-bands. The pattern of fS1 binding was influenced by calcium and fS1 level. Scale bar is 5 μm.

cence was less with ADP than without ADP, and saturated at fS1 levels >2 μM. Differences between high and low calcium were not observed without ADP, but differences were apparent with ADP below 2 nM fS1, with more being bound at pCa 4.0. Comparison of the fluorescence intensity and biochemical data show similar results in that calcium had little influence, (+) ADP gave less bound than (−) ADP, and saturation at fS1 levels was >2 μM.

Analysis of the distribution of fS1 is shown in Fig. 5. For this, the fluorescence intensity was measured in a window in the non-overlap and overlap region, and the ratio of these

was used as a measure of the distribution. A value <1 is obtained when more fS1 is bound in the overlap region, while a value of 2 is obtained when all available actin sites are saturated with fS1 (Swartz et al., 1996). Globally, the ratio saturates with a value of 1.9 at fS1 levels >~2 μM, as observed for sarcomeric intensity and the biochemical assay. Fitting of the data with a sigmoid logistic equation of the form intensity ratio = $((a - d)/(1 + (\text{nM fS1}/c)^b)) + d$ gave the smooth lines in the figure. The fitted values are shown in Table 1 and relate to: a = y-intercept, b = cooperativity parameter, c = total fS1 at the transition
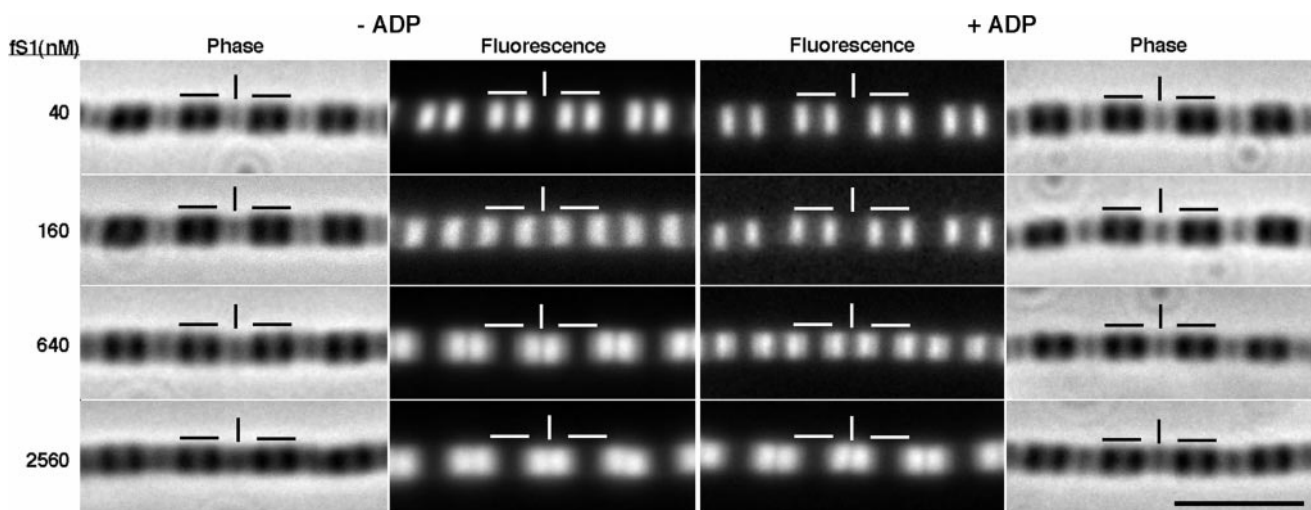

FIGURE 3 The pattern of fS1 binding is influenced by ADP at pCa 9.0. Myofibrils at pCa 9.0 were incubated with different levels of fS1 without (*left two panels*) or with (*right two panels*) 4 mM ADP, fixed, then imaged. Outer panels are phase contrast and inner panels are fluorescence images. The fluorescence images were processed to show fluorescence pattern instead of intensity. Vertical lines note Z-lines and horizontal lines note A-bands. Note the difference in pattern between with and without ADP at 160 and 640 nM fS1. Scale bar is 5 μm.
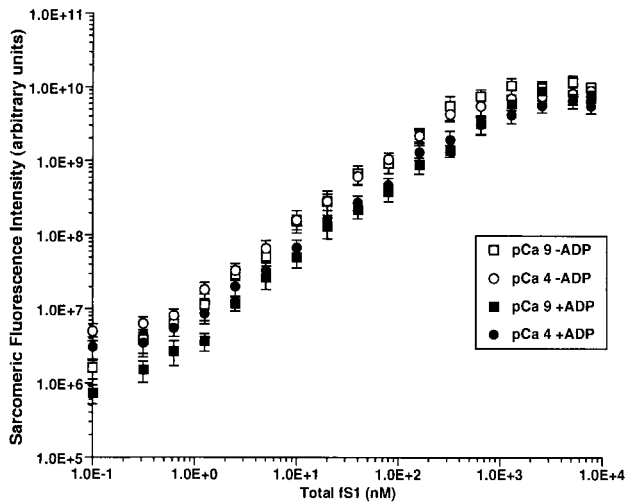
FIGURE 4   Fluorescent S1 binding to myofibrils as measured by fluorescence intensity. Sarcomeric fluorescence intensity was measured as described in Material and Methods and plotted on a log/log scale against total fS1. Data symbols are shown in the inset. There was little difference between pCa 9 and 4 while with ADP resulted in less fS1 bound than without ADP. Data points represent the mean $\pm$ SD (n = 18–20 myofibrils).

TABLE 1   Fitted values for sarcomeric intensity data

Condition	a^*	b^*	c^*	d^*	$r^{2\dagger}$
pCa 9 − ADP	0.26	3.6	227	1.93	0.99
pCa 9 + ADP	0.28	3.2	680	1.90	0.99
pCa 4 − ADP	0.63	1.1	24.3	1.95	0.99
pCa 4 + ADP	0.44	0.84	18.6	1.88	0.99

*sarcomeric intensity = $((a - d)/(1 + (\text{nM fS1}/c)^b)) + d$. a = intensity ratio at 0 fS1; b = cooperativity parameter; c = nM fS1 at midpoint of transition; d = peak plateau intensity ratio.
$^\dagger r^2$ = coefficient of determination.

ranged from 0.63 to 1.9 and was slightly higher than with ADP (0.44 to 1.9) over most of the fS1 range. There was little difference in the transition midpoint for high calcium with and without ADP (18 and 24 nM fS1, respectively). The cooperativity parameter was lower for pCa 4 (0.84 and 1.1, with and without ADP, respectively) than for pCa 9. These data show that calcium had an influence on the distribution of fS1 as a function of fS1 and that ADP had little influence at high calcium and a modest influence at low calcium.

The observation that the bound fS1 saturates at total fS1 levels >2 μM (biochemical and fluorescence microscopy analysis) allows for plotting of the ratio data as a function of sarcomeric fluorescence intensity normalized to 7.68 μM total fS1. This presentation is shown in Fig. 6 and approximates a plot of the distribution as a function of the amount of fS1 bound and corrects for the weaker binding of S1-ADP to the thin filament. The data with and without ADP fit along the same line within the same calcium range. At high calcium the data approximate a hyperbolic function, and at low calcium the data follow a sigmoidal response. This suggests that the changes in the intensity ratio are deter-

midpoint, and d = peak plateau intensity ratio. At pCa 9.0, the ratio was constant ($\sim$0.27) from 0.1 to 100 nM and there was no difference between with and without ADP. Above 100 nM, the ratio changed substantially with small changes in fS1 level (b = 3.6 without ADP and 3.3 with ADP) and this ratio change occurred at lower fS1 without ADP (c = 227 nM fS1) than with ADP (c = 680 nM fS1). At high calcium, the ratio was constant between 0.1 and 1 nM fS1, then increased with increasing fS1. The ratio without ADP
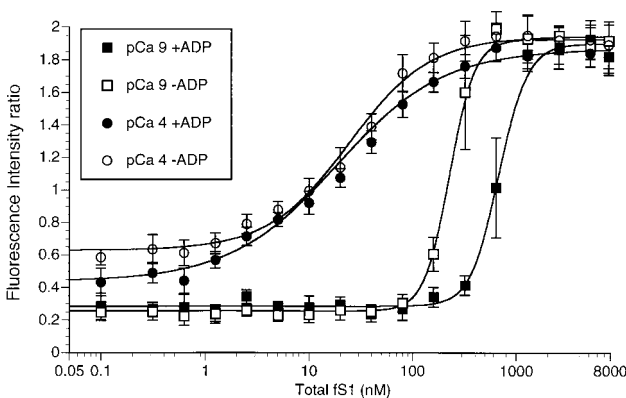

FIGURE 5   Fluorescence intensity ratio at high and low calcium with and without ADP. The fluorescence intensity ratio of non-overlap/overlap was measured as described in Materials and Methods over a wide range of fS1 levels. Data symbols are shown in the inset. The addition of ADP resulted in the same or lower ratio as a function of fS1, and the ratio saturated at fS1 >1 μM at $\sim$2.0. Data points represent the mean $\pm$ SD (n = 18–20 myofibrils).
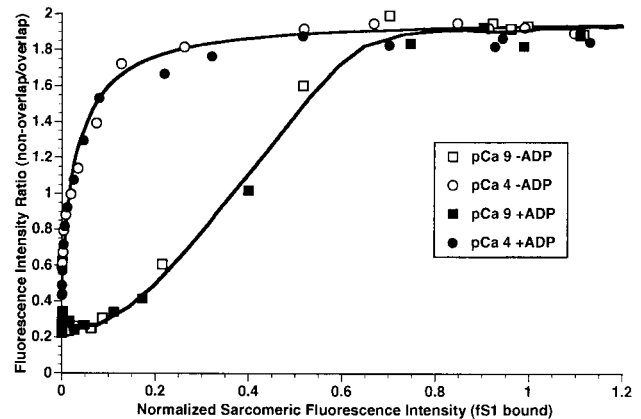

FIGURE 6   Fluorescence intensity ratio as a function of amount bound. The fluorescence intensity ratio is plotted as a function of the amount of fS1 bound (normalized sarcomeric intensity at 7.68 μM fS1). Data symbols are shown in the inset. Note that ADP has little influence on the ratio when plotted in this manner.

mined by the amount of strongly bound fS1 rather than the nucleotide state of the strongly bound fS1.

DISCUSSION

Methods were developed to measure the amount and distribution of strong-binding myosin heads to the regulated actin filaments of myofibrils using quantitative digital fluorescence microscopy (Swartz et al., 1996). This allows for monitoring the state of the thin filament by analysis of the distribution of fS1 within the sarcomere. The current study expanded the previous work by using a larger data base and a more robust analysis. These methods were further confirmed by comparing sarcomeric fluorescence intensity with biochemical measures of bound fS1. A direct correlation between the biochemical and fluorescence intensity is not readily doable, as the biochemical assay directly measures the free fS1 (bound by difference) while the fluorescence intensity directly measures bound fS1. Also, the biochemical assay had much larger errors than the intensity measurements. Despite these difficulties, comparisons can be made between the trends in the data. Both assays showed the same trends in terms of the influence of calcium and ADP on the amount of fS1 bound as well as saturation as a function of total fS1 level. This suggests that the fluorescence intensity measurements are related to the amount and distribution of fS1 rather than quenching of the fluorophore linked to the S1.

The data can be interpreted with the two-state model developed by Hill et al. (1980) or the three-state model developed by Geeves and colleagues (McKillop and Geeves, 1993; Head et al., 1995; Maytum et al., 1999). Both models postulate that calcium and strong S1 binding shift the thin filament into the open/on state and that this transition is independent of the nucleotide bound to S1. Our studies cannot readily support one model over the other, as the blocked state was defined from kinetic studies (McKillop and Geeves, 1993). We prefer to interpret our data from the three-state model, as there are kinetic (Head et al., 1995) and structural (Vibert et al., 1997) data that support this model. The three states are blocked, closed, and open, and the overlap and non-overlap regions of the thin filament can be in any of these states, depending on conditions. The fS1 does not bind the blocked state and is not detected with our methods. We assume that with or without ADP, and high or low calcium, the overlap region is in the open state because there are intrinsic myofibrillar cross-bridges strongly bound to the thin filament. We also assume that the fS1 detected is bound to actin sites in the open state rather than the closed state. This assumption is based upon the observation that K_2 (isomerization into the strong-binding open state) is 200 without ADP and 20 with ADP (Maytum et al., 1999). A 10-fold difference should result in more of the attached fS1 (both weakly and strongly bound) being in the non-overlap region with ADP than without ADP, resulting in higher intensity ratios for with ADP than without ADP. This was not observed (Fig. 5).

The state of the non-overlap region is calcium- and fS1 level-dependent and can be monitored relative to the open state in the overlap region using the fluorescence intensity ratio. At low calcium and low fS1, the non-overlap region is predominantly in the blocked state. At high calcium and low fS1, the non-overlap region is predominantly in the closed state. At saturating fS1, this region of the thin filament is in the open state independent of calcium. By monitoring the distribution of fS1 using the fluorescence intensity ratio as a function of fS1 level at high and low calcium and with and without ADP, we can further test the model within the intact filament lattice to determine if the nucleotide state of the strongly bound cross-bridge influences activation of the thin filament.

The intensity ratio, in theory, should range from near 0 to 2.0 using the three-state model and the density of available actin binding sites in the overlap and non-overlap region (Swartz et al., 1996). Relating the intensity ratio to the fraction of open actin sites can be done by halving the intensity ratio. Hence, if all actins are in the open state, the intensity ratio is 2.0 (1.0 fraction of open actin sites). Under conditions that should result in all actins being in the open state (primarily high fS1 levels), the curve-fitting gave a plateau of 1.9 (0.9 fraction of open actin sites), very close to the predicted value. The presence of the open state in the overlap region independent of calcium or ADP is interpreted from the intensity data that show values <1 at low fS1 (more fS1 in the overlap region, Fig. 5). There is a preference for the fS1 to bind in this region because it has the highest affinity (open state) for the fS1.

At the extreme of very low fS1, the y-intercept values (Fig. 5) support the model in that they can be related to the distribution of open actin sites as influenced by calcium alone. At low calcium, the non-overlap region is primarily in the blocked and closed state; at high calcium, the non-overlap region is primarily in the closed state, with some sites in the open state. This influence of calcium is shown by the difference in the y-intercepts pCa 9 and 4 (Fig. 5). The fraction of closed and open states is estimated at 0.22 and 0.02, respectively without calcium, while it is 0.80 and 0.20 with calcium (McKillop and Geeves, 1993). A minimum of 0.26 (0.13 fractional saturation) was obtained from curve-fitting of the data at pCa 9.0. If fS1 was bound only to the open sites, the intensity ratio would be 0.04 without calcium. This is about sixfold lower than the observed intensity ratio. This difference can be expected because of the nature of light emission from a fluorophore and the spatial resolution of the methods. It is assumed that the higher value is caused by light emitted from fS1 in the overlap region. If the region of interest for the non-overlap region were moved closer to the Z-line, then the y-intercept value would be lower. An alternative explanation is that attached fS1 (via formaldehyde fixation) is bound at both open and closed

sites. If this were the case, then the *y*-intercept intensity ratio should be 0.48 [(0.22 + 0.02)x2]; ~2-fold higher than that observed. While this could explain the observation, the arguments for the fS1 detected being that bound to the open state (described above) do not favor this, nor do the data for pCa 4.0. If our method of measurement is not the reason for the difference between the biochemical data and our data, then our data at low calcium do not support the three-state model.

The *y*-intercept was higher for pCa 4 than 9, supporting the hypothesis that calcium alters the equilibrium among the three states (McKillop and Geeves, 1993). Biochemical data suggest that calcium alters the equilibrium among the three states such that the closed state predominates at high calcium with 80–85% of the actin being in the closed state, and the remaining 15–20% being in the open state (Maytum et al., 1999). Converting these proportions into intensity ratio values give 0.3–0.4 for the open state. The *y*-intercept for pCa 4 with ADP was 0.44, in strong agreement with the biochemical data. Without ADP and at pCa 4, the intercept was 0.63 (0.31 actin sites), which is not in strong agreement with the biochemical data in absolute terms. In relative terms, it is in agreement in that calcium alone does not shift all actin sites into the open or active state because the intensity ratio was <1. If the attached fS1 was bound to both open and closed states, then the *y*-intercept would be 2 [(0.8 + 0.2)x2]. This was not the case, which further supports the assumption that the attached fS1 was bound to open sites. The difference between the *y*-intercepts for with and without ADP at high calcium suggests that the nucleotide state of fS1 may have a minor influence upon the closed to open equilibrium. However, in this low fS1 range, the images are difficult to analyze and the data are more noisy.

The increases in the intensity ratio with increased fS1 were gradual at high calcium and very steep at low calcium. Both of these changes are congruent with the three-state model in that the binding of the fS1 shifts the actin to the open or active state. The cooperativity parameter (steepness of the fS1/intensity ratio relationship) determined from curve-fitting was greater without calcium than with, which is a feature observed in biochemical studies (Maytum et al., 1999). However, we did not observe apparent cooperativity at high calcium that is observed in solution (Maytum et al., 1999). At high calcium, some of the sites (~20% in the non-overlap region) are in the open state, and thus become occupied with fS1 even at very low fS1 (Fig. 5). The lack of apparent cooperativity with calcium could be because of a difference in the native myofibrillar thin filament compared to the reconstituted thin filament and/or our method of measurement and analysis compared to the solution studies. At low calcium, the transition was very steep. This is expected because the non-overlap actin is primarily in the blocked state. The fS1 fills the overlap actin sites first, then binds in the non-overlap region nearest the A-band/I-band

junction and likely propagates toward the Z-line (Swartz et al., 1990, 1996). Thus, the actin sites shift from the blocked to closed to open state. Whether the actin can shift from the blocked state directly to the open state cannot be addressed with our methods.

A feature of the two- and three-state models is that the nucleotide state of the strong binding cross-bridge does not influence the closed (off)/open (on) transition (Hill et al., 1980; Maytum et al., 1999). This feature has been supported by biochemical studies (Greene, 1982; Maytum et al., 1999). Our studies on fS1 binding to the myofibrillar thin filament show that, at very low levels of fS1, ADP has no influence on the distribution at low calcium and has a small effect at high calcium, with (−) ADP having a greater value for the *y*-intercept, suggesting a minor influence of cross-bridge state upon the closed-to-open transition (Fig. 5). However, when the data are plotted in relative terms to show the change in distribution as a function of amount of fS1 bound, there is little difference in the change in distribution as a function of relative sarcomeric intensity (Fig. 6). This plot emphasizes intermediate-to-high levels of fS1 rather than the low level fS1, as shown in Fig. 5. From the data plotted in Fig. 6 we infer that the transition from the closed to open state is dependent upon the number of strongly bound cross-bridges rather than the state of the cross-bridge in agreement with the solution binding studies. If the nucleotide state had a significant influence on the transition from closed to open state, then the coincidence of the with and without ADP intensity data as a function of relative sarcomeric intensity would not be apparent. Studies on the geometry of the S1/actin interaction with and without ADP suggest no difference in the position of the S1 in skeletal muscle, while smooth muscle S1 did show a difference (Gollub et al., 1996). These observations also fit with our observations on the influence of ADP on fS1 binding.

Other studies using mechanical measurements suggest that ADP cross-bridges are more effective at activating actin than nucleotide-free cross-bridges (Thirlwell et al., 1994; Horiuti et al., 1997; Yamaguchi, 1998), which does not agree with our interpretations on how ADP influences fS1 binding. These studies used either low MgATP to induce calcium-free contraction (Yamaguchi, 1998) or measured-tension transients after release of caged ATP (Thirlwell et al., 1994; Horiuti et al., 1997). In all cases, addition of ADP enhanced the steady-state force or amplitude of the tension transient. This led to the conclusion that either ADP cross-bridges are more effective activators of the thin filament (Yamaguchi, 1998) or that ADP cross-bridges promote cooperative activation of the thin filament, whereas nucleotide-free cross-bridges do not (Thirlwell et al., 1994). Our studies and the biochemical studies suggest that ADP does not influence thin filament activation as measured by binding, while the mechanical studies suggest that ADP cross-bridges are more effective activators than nucleotide-free

cross-bridges as measured by force generation. This difference may be real in that ADP cross-bridges may be more effective at activating force generation than binding. More sophisticated probes for measuring thin filament activation in myofibrils or skinned fibers are needed to address this issue.

In conclusion, our data show that activation of the thin filament (as measured by fS1 binding) is primarily dependent upon the number of strongly bound cross-bridges and not their nucleotide state, in agreement with the McKillop and Geeves three-state and Hill two-state models. They also support the concept that a major component of the activation process is the binding of strong cross-bridges to the thin filament rather than calcium (Lehrer, 1994).

REFERENCES

Brenner, B. 1988. Effect of Ca^{2+} on crossbridge turnover kinetics in skinned single rabbit psoas fibers: implications for regulation of muscle contraction. *Proc. Natl. Acad. Sci. U.S.A.* 85:3265–3269.

Brenner, B., and J. M. Chalovich. 1999. Kinetics of thin filament activation probed by fluorescence of *N*-((2-iodoacetoxy)ethyl)-*N*-methyl-7-nitrobenz-2-oxo-1,3-diazole-labeled troponin I incorporated into skinned fibers of rabbit psoas muscle: implications for regulation of muscle contraction. *Biophys. J.* 77:2691–2708.

Brenner, B., T. Kraft, L. C. Yu, and J. M. Chalovich. 1999. Thin filament activation probed by fluorescence of *N*-((2-iodoacetoxy)ethyl)-*N*-methyl-7-nitrobenz-2-oxo-1,3-diazole-labeled troponin I incorporated into skinned fibers of rabbit psoas muscle. *Biophys. J.* 77:2677–2691.

Carter, S. G., and D. W. Karl. 1982. Inorganic phosphate assay with malachite green: an improvement and evaluation. *J. Biochem. Biophys. Methods*. 7:7–13.

Chalovich, J. M. 1992. Actin mediated regulation of muscle contraction. *Pharmacol. Ther*. 55:95–148.

Chalovich, J. M., and E. Eisenberg. 1982. Inhibition of actomyosin ATPase activity by troponin-tropomyosin without blocking the binding of myosin to actin. *J. Biol. Chem.* 257:2432–2437.

Fabiato, A. 1988. Computer programs for calculating total from specified free or free from specified total ionic concentrations in aqueous solutions containing multiple metals and ligands. *Methods Enzymol*. 157:378–417.

Farah, C. S., and F. C. Reinach. 1999. Regulatory properties of recombinant tropomyosins containing 5-hydroxytryptophan: Ca^{2+}-binding to troponin results in a conformational change in a region of tropomyosin outside the troponin binding site. *Biochemistry*. 38:10543–10551.

Godt, R. E., and B. D. Lindley. 1982. Influence of temperature upon contractile activation and isometric force production in mechanically skinned muscle fibers of the frog. *J. Gen. Physiol*. 80:279–297.

Gollub, J., C. R. Cremo, and R. Cooke. 1996. ADP release produces a rotation of the neck region of smooth myosin but not skeletal myosin. *Nat. Struct. Biol*. 3:796–802.

Gordon, A. M., M. A. LaMadrid, Y. Chen, Z. Luo, and P. B. Chase. 1997. Calcium regulation of skeletal muscle thin filament motility in vitro. *Biophys. J.* 72:1295–1307.

Gornall, A. G., C. J. Bardawill, and M. M. David. 1949. Determination of serum protein by means of the biuret reaction. *J. Biol. Chem*. 177:751–766.

Graceffa, P. 1999. Movement of smooth muscle tropomyosin by myosin heads. *Biochemistry*. 38:11984–11992.

Greene, L. E. 1982. Effect of nucleotide on the binding of S1 to regulated actin. *J. Biol. Chem*. 257:2432–2437.

Head, J. G., M. D. Ritchie, and M. A. Geeves. 1995. Characterization of the equilibrium between blocked and closed states of muscle thin filaments. *Eur. J. Biochem*. 227:694–699.

Hill, T. L., E. Eisenberg, and L. E. Greene. 1980. Theoretical model for the cooperative equilibrium binding of myosin subfragment 1 to the actin-troponin-tropomyosin complex. *Proc. Natl. Acad. Sci. U.S.A.* 77:3186–3190.

Hill, H. D., and J. G. Straka. 1988. Protein determination using bicinchoninic acid in the presence of sulfhydryl reagents. *Anal. Biochem.* 170:203–208.

Homsher, E., B. Kim, A. Bobkova, and L. S. Tobacman. 1996. Calcium regulation of thin filament movement in an in vitro motility assay. *Biophys. J.* 70:1881–1892.

Horiuti, K., N. Yagi, and S. Takemori. 1997. Mechanical study of rat soleus muscle using caged ATP and x-ray diffraction: high ADP affinity of slow cross-bridges. *J. Physiol*. 502.2:443–447

Ishii, Y., and S. S. Lehrer. 1990. Eximer fluorescence of pyrenyliodoacetamide-labeled tropomyosin: A probe of the state of tropomyosin in reconstituted muscle thin filaments. *Biochemistry*. 29:1160–1166.

Lehman, W., R. Craig, and P. Vibert. 1994. Ca^{2+}-induced tropomyosin movement in Limulus thin filaments revealed by three-dimensional reconstruction. *Nature*. 368:65–67.

Lehrer, S. S. 1994. The regulatory switch of the muscle thin filament: Ca^{2+} or myosin heads. *J. Muscle. Res. Cell Motil*. 15:232–236.

Maytum, R., S. S. Lehrer, and M. A. Geeves. 1999. Cooperativity and switching within the three-state model of muscle regulation. *Biochemistry*. 38:1102–1110.

McKillop, D. F. A., and M. A. Geeves. 1991. Regulation of the actomyosin subfragment 1 interaction by troponin/tropomyosin. *Biochem. J.* 279:711–718.

McKillop, D. F. A., and M. A. Geeves. 1993. Regulation of the interaction between actin and myosin subfragment 1: Evidence for three states of the thin filament. *Biophys. J.* 65:693–701.

Miki, M., and T. Iio. 1993. Kinetics of structural changes of reconstituted skeletal muscle thin filaments observed by fluorescence resonance energy transfer. *J. Biol. Chem*. 268:7101–7106.

Miki, M., T. Miura, K.-I. Sano, H. Kimura, H. Kondo, H. Ishida, and Y. Maéda. 1998. Fluorescence resonance energy transfer between points on tropomyosin and actin in skeletal muscle thin filaments: Does tropomyosin move? *J. Biochem*. 123:1104–1111.

Millar, N., and E. Homsher. 1990. The effect of phosphate and calcium on force generation in glycerinated rabbit skeletal muscle fibers. *J. Biol. Chem*. 265:20234–20240.

Popp, D., and Y. Maéda. 1993. Calcium ions and the structure of muscle actin filament. An x-ray diffraction study. *J. Mol. Biol*. 229:279–285.

Squire, J. M., and E. P. Morris. 1998. A new look at thin filament regulation in vertebrate muscle. *FASEB J*. 12:761–771.

Swartz, D. R., M. L. Greaser, and B. B. Marsh. 1990. Regulation of binding of subfragment 1 in isolated rigor myofibrils. *J. Cell Biol*. 111:2989–3001.

Swartz, D. R., and R. L. Moss. 1992. Influence of a strong binding myosin analog on Ca^{2+}-sensitive mechanical properties of skinned skeletal muscle fibers. *J. Biol. Chem*. 267:20497–20506.

Swartz, D. R., R. L. Moss, and M. L. Greaser. 1996. Calcium alone does not fully activate the thin filament for S1 binding to rigor myofibrils. *Biophys. J.* 71:1891–1904.

Swartz, D. R., R. L. Moss, and M. L. Greaser. 1997. Characteristics of TnC binding to the myofibrillar thin filament: Extraction of TnC is not random along the length of the thin filament. *Biophys. J.* 73:293–305.

Swartz, D. R., D. Zhang, and K. W. Yancey. 1999. Crossbridge-dependent activation of contraction in cardiac myofibrils at low pH. *Am. J. Physiol. Heart Circ. Physiol.* 276:H1460–H1467.

Tao, T., B.-J. Gong, and P. C. Leavis. 1990. Calcium-induced movement of troponin-I relative to actin in skeletal muscle thin filaments. *Science.* 247:1339–1341.

Tao, T., M. Lamkin, and S. S. Lehrer. 1983. Excitation energy transfer studies of the proximity between tropomyosin and actin in reconstituted skeletal muscle thin filaments. *Biochemistry.* 22:3059–3066.

Thirlwell, H., J. T. Corrie, G. P. Reid, D. R. Trentham, and M. A. Ferenczi. 1994. Kinetics of relaxation from rigor or permeabilized fast-twitch skeletal fibers from the rabbit using a novel caged ATP and apyrase. *Biophys. J.* 67:2436–2447.

Vibert, P., R. Craig, and W. Lehman. 1997. Steric model for activation of muscle thin filaments. *J. Mol. Biol*. 266:8–14.

Walker, J. W., Z. Lu, and R. L. Moss. 1992. Effects of Ca^{2+} on the kinetics of phosphate release in skeletal muscle. *J. Biol. Chem*. 267:2459–2466.

Xu, C., R. Craig, L. Tobacman, R. Horowitz, and W. Lehman. 1999. Tropomyosin positions in regulated thin filaments revealed by cryoelectron microscopy. *Biophys. J.* 77:985–992.

Yamaguchi, M. 1998. Modulating factors of calcium-free contraction at low [MgATP]: a physiological study on the steady states of skinned fibers of frog skeletal muscle. *J. Muscle Res. Cell Motil*. 19:949–960.